High-p_T results and parton density functions from ATLAS.

Javier Llorente
on behalf of the ATLAS Collaboration.

Simon Fraser University

QCD @ work 2022 - June 28, 2022

Introduction

- The QCD cross section can be factorised in three parts: IS, HS, FS.
- The ATLAS Collaboration has published important QCD results recently.
- Measurements are exploited to understand these three parts separately.

- Initial State $\Rightarrow$ Parton Density $f_i(x, \mu_F)$
- Hard Scattering $\Rightarrow$ Matrix Element $\hat{\sigma} \propto |\mathcal{M}|^2$
- Final State $\Rightarrow$ Fragm. Functions $D_a^h(z, Q^2)$

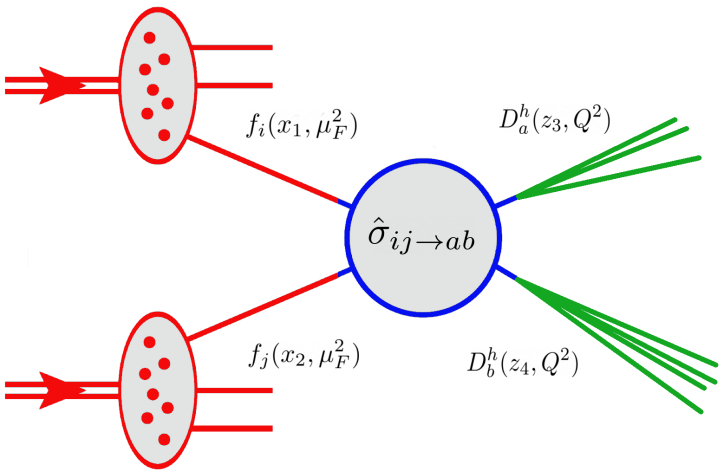

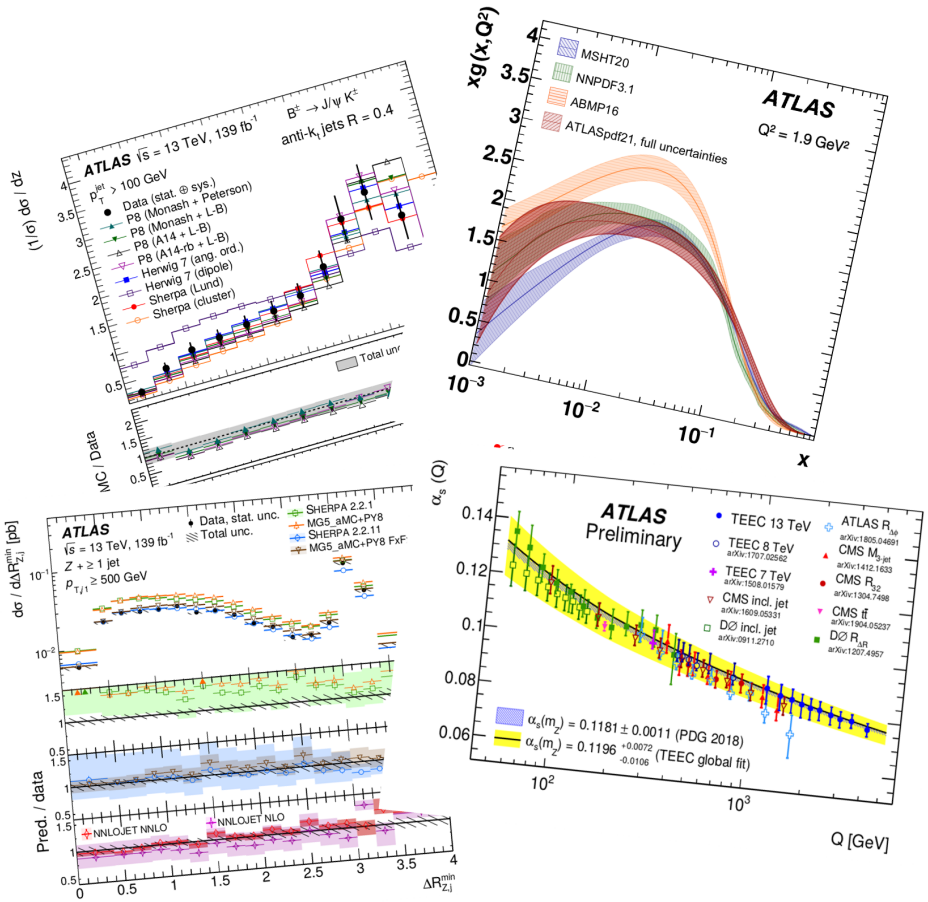

$$d\sigma = \sum_{i,j,a,b} \int_{\Omega} d^2\vec{x} d^2\vec{z}\, f_i(x_1, \mu_F^2) f_j(x_2, \mu_F^2) \times d\hat{\sigma}_{ij\to ab}(\vec{x}, \mu_R^2) \times D_a^h(z_3, Q^2) D_b^h(z_4, Q^2)$$

ATLAS global PDF fit at $\sqrt{s} = 7, 8, 13$ TeV [EPJC 82, 438 (2022)]

- Determination of parton distribution functions using HERA + ATLAS data.
- Multiple datasets used at different pp centre-of-mass energies $\sqrt{s} = 7, 8, 13$ TeV.
- Theoretical predictions at NNLO QCD + NLO EW (current state-of-the-art).
- Uncertainties on (μ_R, μ_F) treated as correlated in the fit where they are sizeable with respect to experimental systematics.
- Detailed study of correlations between different ATLAS datasets.
- Extended PDF parameterisation using 21 parameters.

Data set	$\sqrt{s}$ [TeV]	Luminosity [fb^{-1}]	Decay channel	Observables entering the fit
Inclusive $W, Z/\gamma^*$	7	4.6	e, μ combined	η_ℓ (W), y_Z (Z)
Inclusive Z/γ^*	8	20.2	e, μ combined	$\cos\theta^*$ in bins of $y_{\ell\ell}$, $m_{\ell\ell}$
Inclusive W	8	20.2	μ	η_μ
$W^\pm$ + jets	8	20.2	e	p_{T}^W
Z + jets	8	20.2	e	$p_{\mathrm{T}}^{\mathrm{jet}}$ in bins of $\lvert y^{\mathrm{jet}}\rvert$
$t\bar{t}$	8	20.2	lepton + jets, dilepton	$m_{t\bar{t}}$, p_{T}^t, $y_{t\bar{t}}$
$t\bar{t}$	13	36	lepton + jets	$m_{t\bar{t}}$, p_{T}^t, y_t, $y_{t\bar{t}}^{\mathrm{b}}$
Inclusive isolated γ	8, 13	20.2, 3.2	-	E_{T}^γ in bins of η^γ
Inclusive jets	7, 8, 13	4.5, 20.2, 3.2	-	$p_{\mathrm{T}}^{\mathrm{jet}}$ in bins of $\lvert y^{\mathrm{jet}}\rvert$

ATLAS global PDF fit at $\sqrt{s} = 7$, 8, 13 TeV [EPJC 82, 438 (2022)]

- Comparison to global PDF sets (CT18, NNPDF, MSHT20, ...)
- Inclusion of ATLAS data brings ATLAS PDF closer to global PDF sets than to HERAPDF.
- Measurement of $R_s(x, Q^2) = x(s + \bar{s})/x(\bar{u} + \bar{d})$.
- Uncertainties estimated using different tolerances $T = \sqrt{\Delta\chi^2} = 1, 3$.

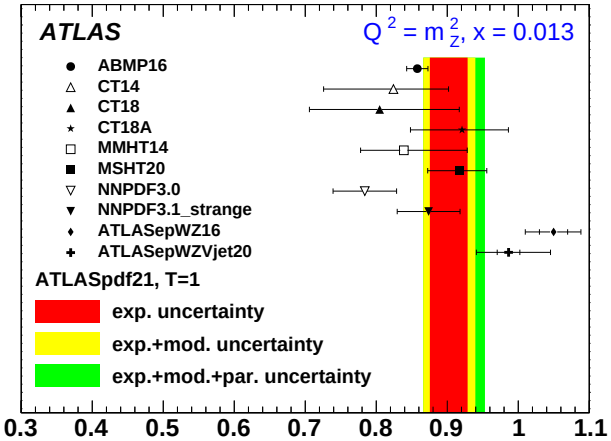

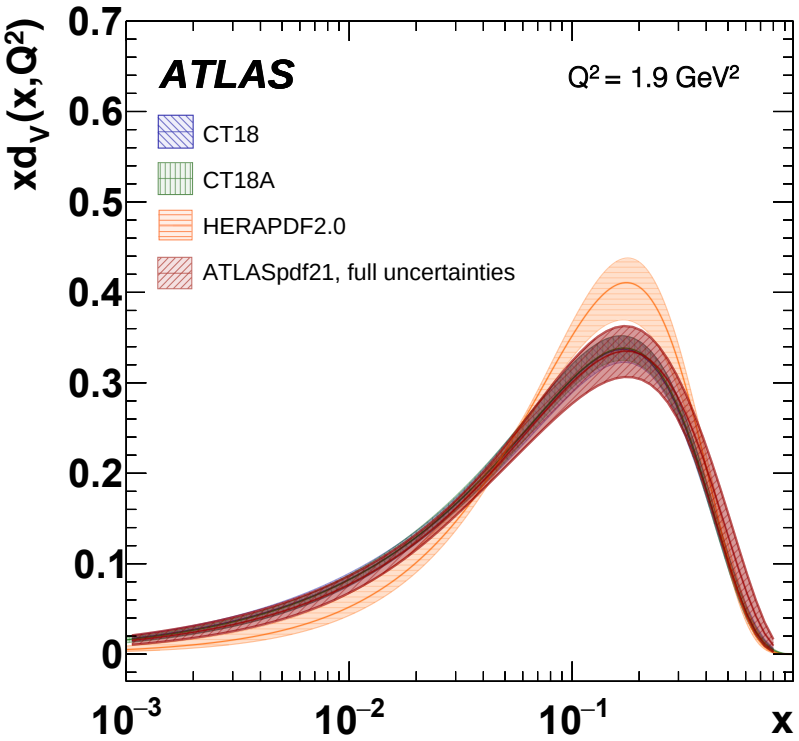

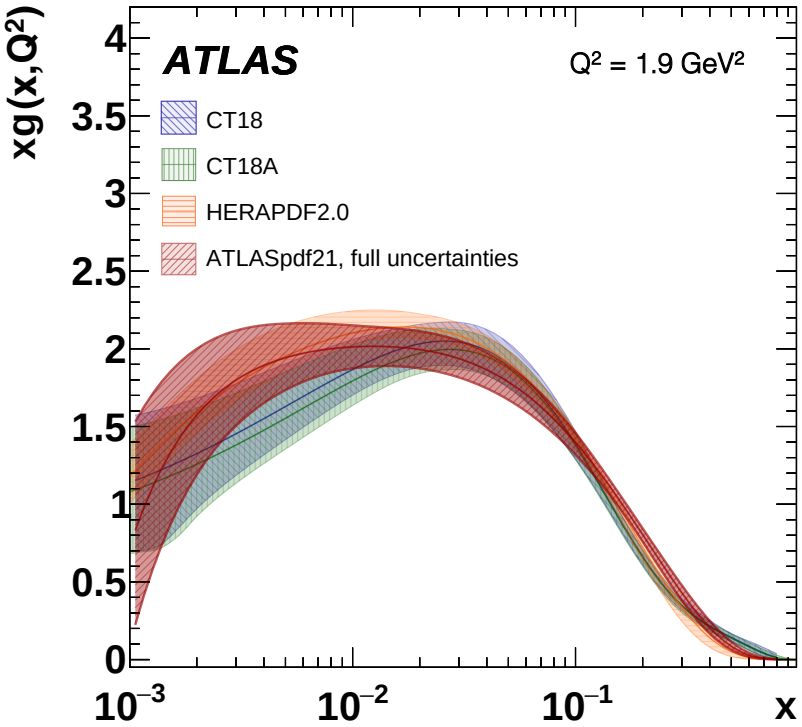

ATLAS Z-boson + high-p_T jets at $\sqrt{s} = 13$ TeV [arXiv:2205.02597]

- $Z \to ee$ ($\mu\mu$) with additional jets ($p_T > 100$ GeV).
- High-p_T region is selected with $p_T^{\text{jet}} > 500$ GeV.
- Z-boson radiation $\propto \alpha_s \ln^2(p_{T,j_1}/m_Z)$.

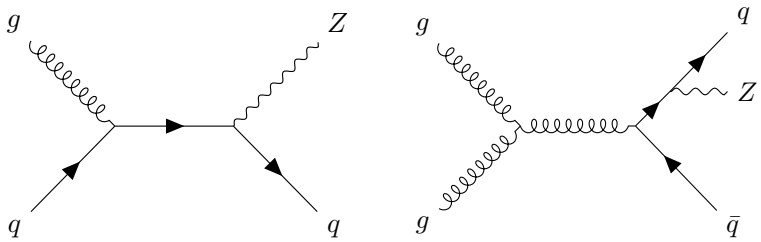

- Different angular topologies studied using $\Delta R_{Zj} = \sqrt{\Delta y_{Zj}^2 + \Delta\phi_{Zj}^2}$.
- Comparison to different ME+PS and fixed-order predictions.

Inclusive

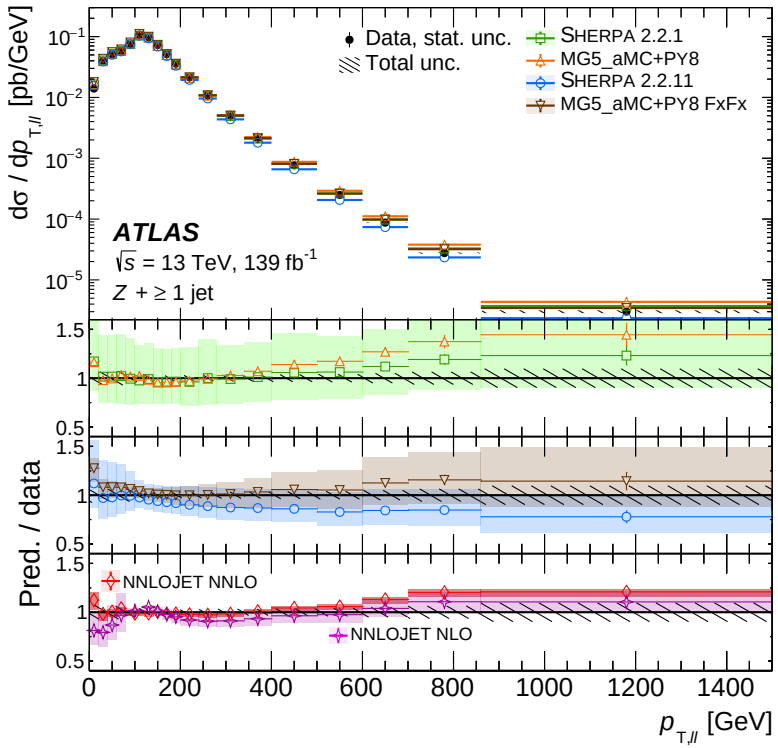

High-p_T

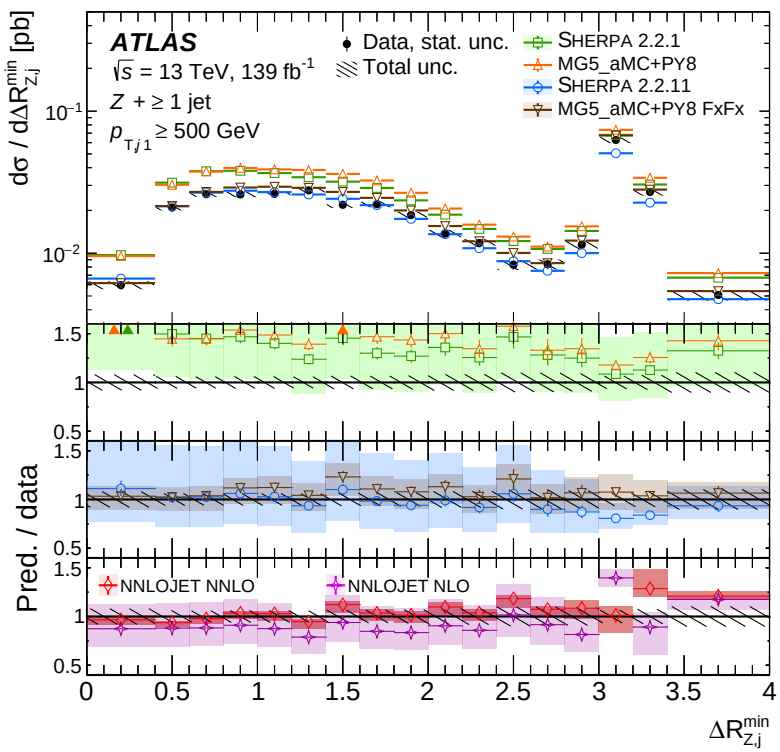

ATLAS Z-boson + high-p_T jets at $\sqrt{s} = 13$ TeV [arXiv:2205.02597]

- Measurement of $r_{Zj} = \dfrac{p_{T,\ell\ell}}{p_T(\text{closest jet})}$ in ΔR bins.
- Excellent description by NNLO QCD + NLO EW.
- Sherpa 2.2.1 and MG5_aMC+Py8 overestimate the cross section at high p_T.
- Sherpa 2.2.11 and FxFx merging for MG5_aMC+Py8 provide an improved description.

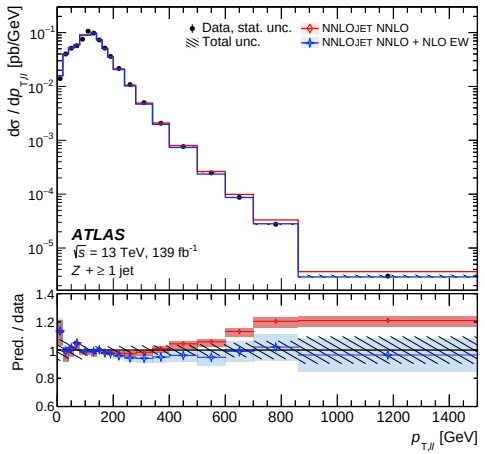

Collinear

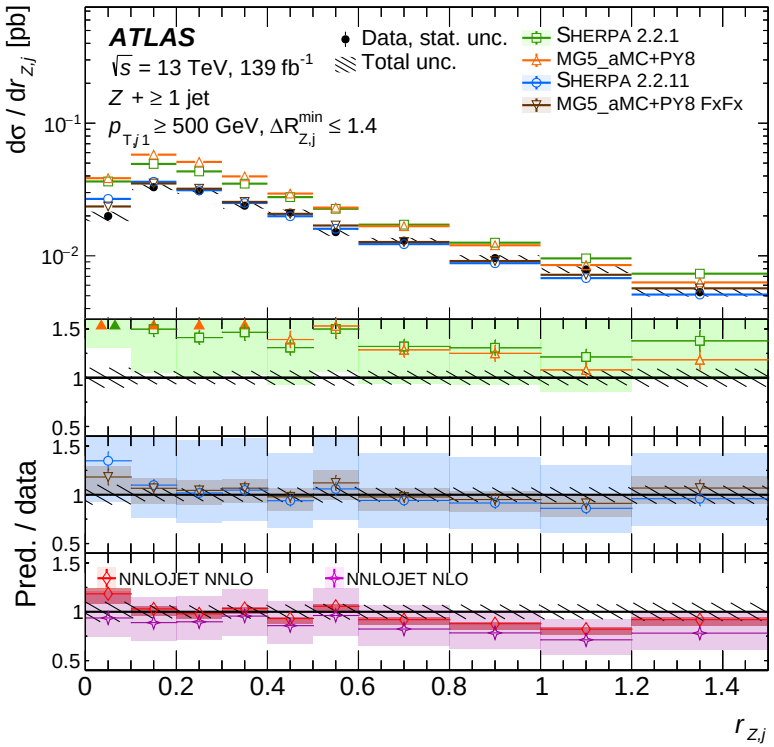

Back-to-back

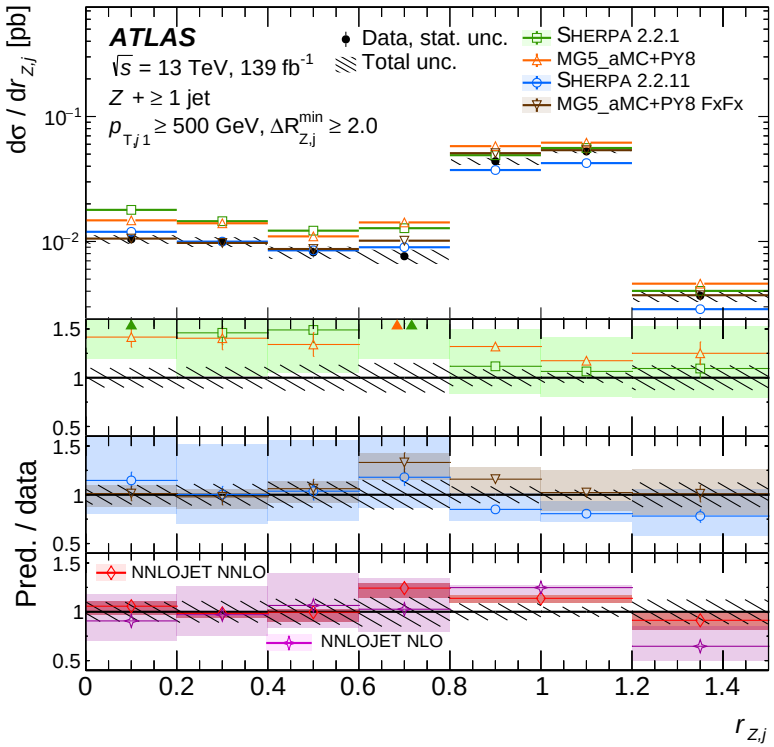

Measurement of TEEC at $\sqrt{s} = 13$ TeV [ATLAS-CONF-2020-025]

TEEC: The x_{T}-weighted distribution of differences in azimuth between jets i and j, with $x_{\mathrm{T}i} = \frac{E_{\mathrm{T}i}}{\sum_k E_{\mathrm{T}k}}$

$$\frac{1}{\sigma}\frac{d\Sigma}{d(\cos\phi)} = \frac{1}{\sigma}\sum_{ij}\int \frac{d\sigma}{dx_{\mathrm{T}i}dx_{\mathrm{T}j}d(\cos\phi)} x_{\mathrm{T}i}x_{\mathrm{T}j}dx_{\mathrm{T}i}dx_{\mathrm{T}j}$$

And the azimuthal asymmetry ATEEC is defined as

$$\frac{1}{\sigma}\frac{d\Sigma^{\mathrm{asym}}}{d(\cos\phi)} \equiv \frac{1}{\sigma}\frac{d\Sigma}{d(\cos\phi)}\bigg|_{\phi} - \frac{1}{\sigma}\frac{d\Sigma}{d(\cos\phi)}\bigg|_{\pi-\phi}$$

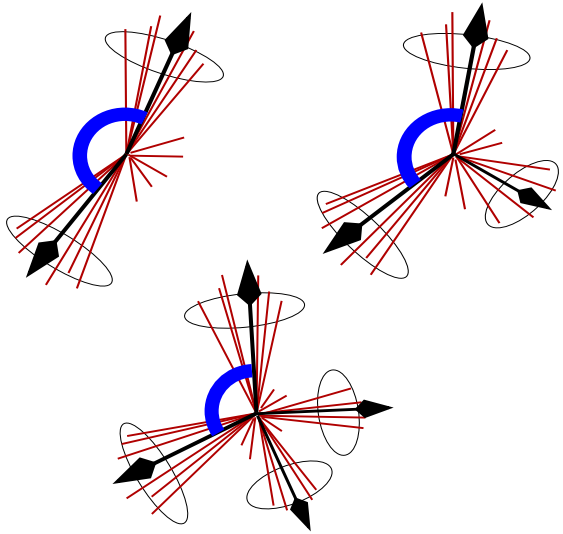

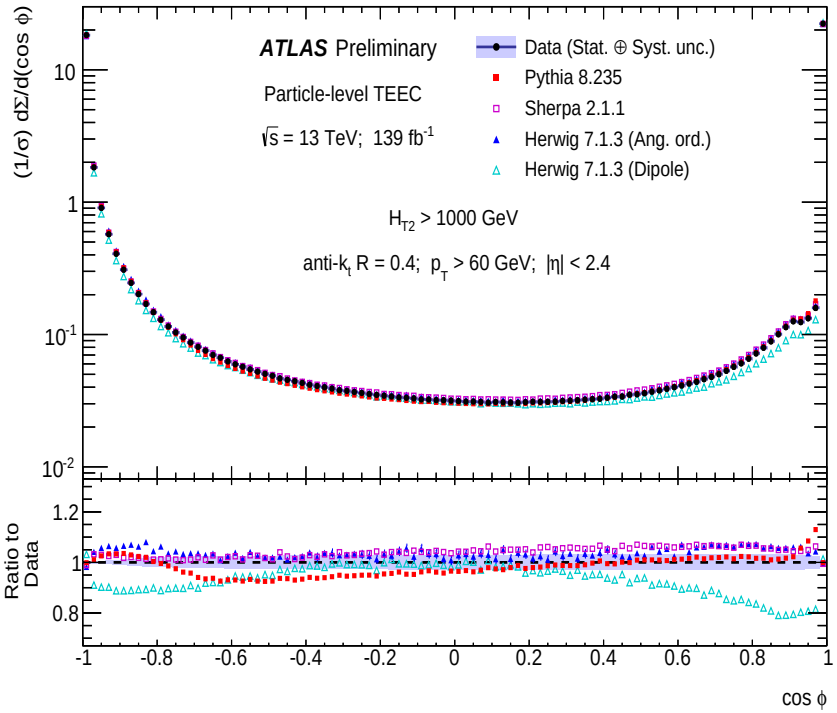

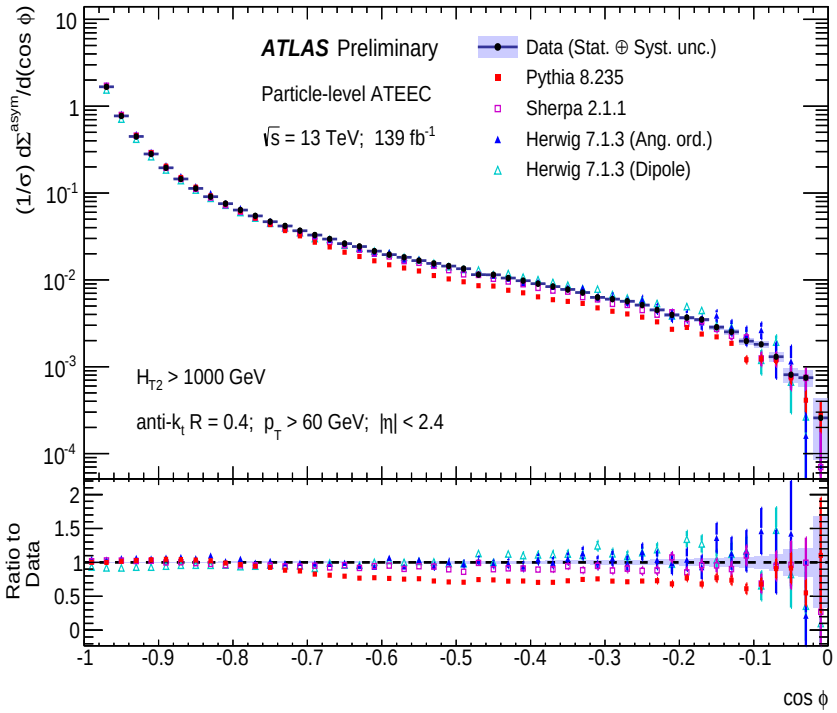

Measurement of TEEC at $\sqrt{s} = 13$ TeV [ATLAS-CONF-2020-025]

Comparison of TEEC (left) and ATEEC (right) with NLO predictions ($\mu = \hat{H}_T$)

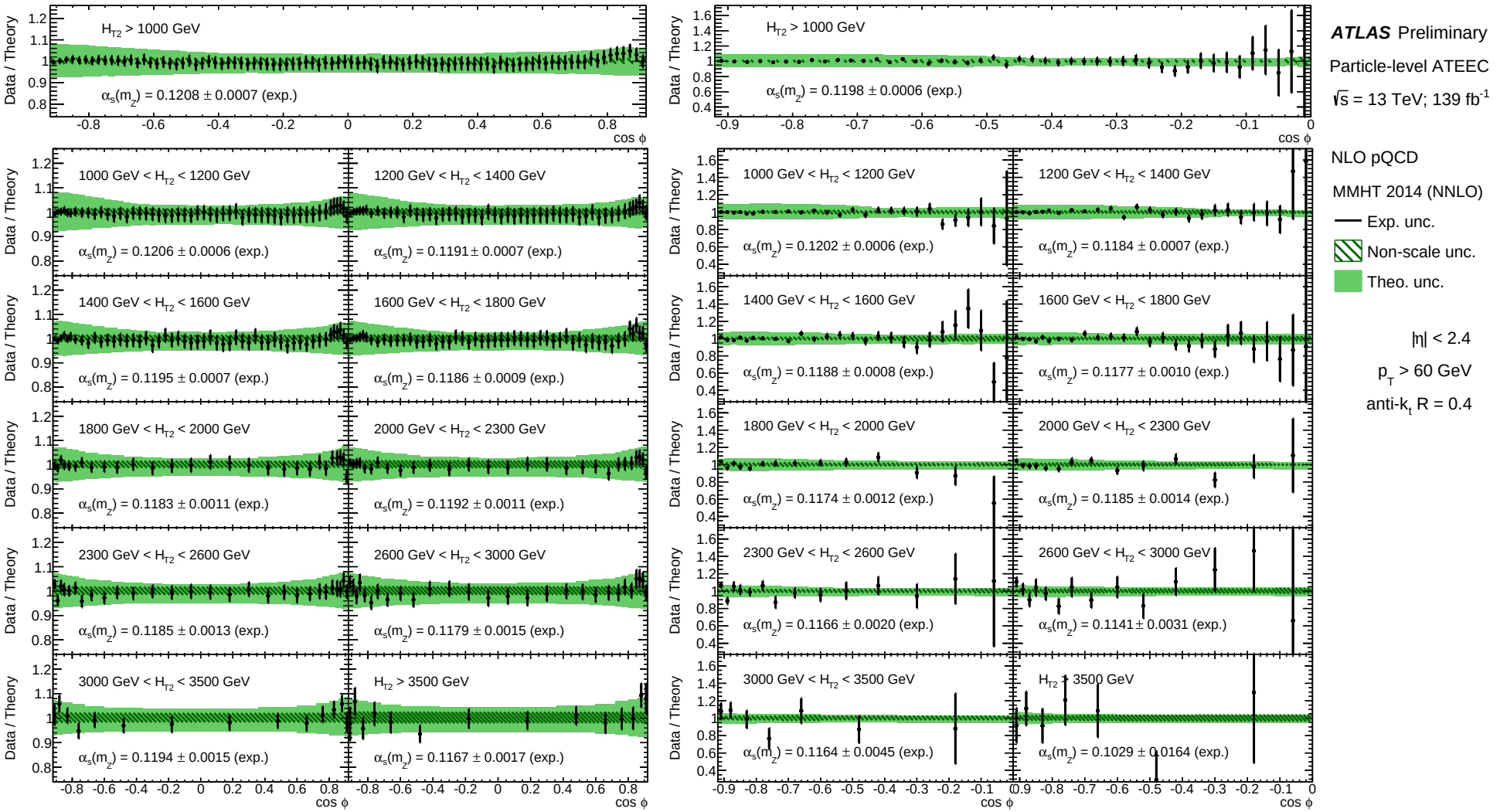

Non-perturbative corrections of $\mathcal{O}(1\%)$. Very good data / theory agreement.

Measurement of TEEC at $\sqrt{s} = 13$ TeV [ATLAS-CONF-2020-025]

- $\alpha_s(Q)$ is determined by minimizing a $\chi^2(\alpha_s, \vec{\lambda})$ function for each H_{T2} bin.

$$\chi^2(\alpha_s, \vec{\lambda}) = \sum_i \frac{[x_i - F_i(\alpha_s, \vec{\lambda})]^2}{\Delta x_i^2 + \Delta \xi_i^2} + \sum_k \lambda_k^2; \qquad F_i(\alpha_s, \vec{\lambda}) = \psi_i(\alpha_s)\left(1 + \sum_k \lambda_k \sigma_k^{(i)}\right)$$

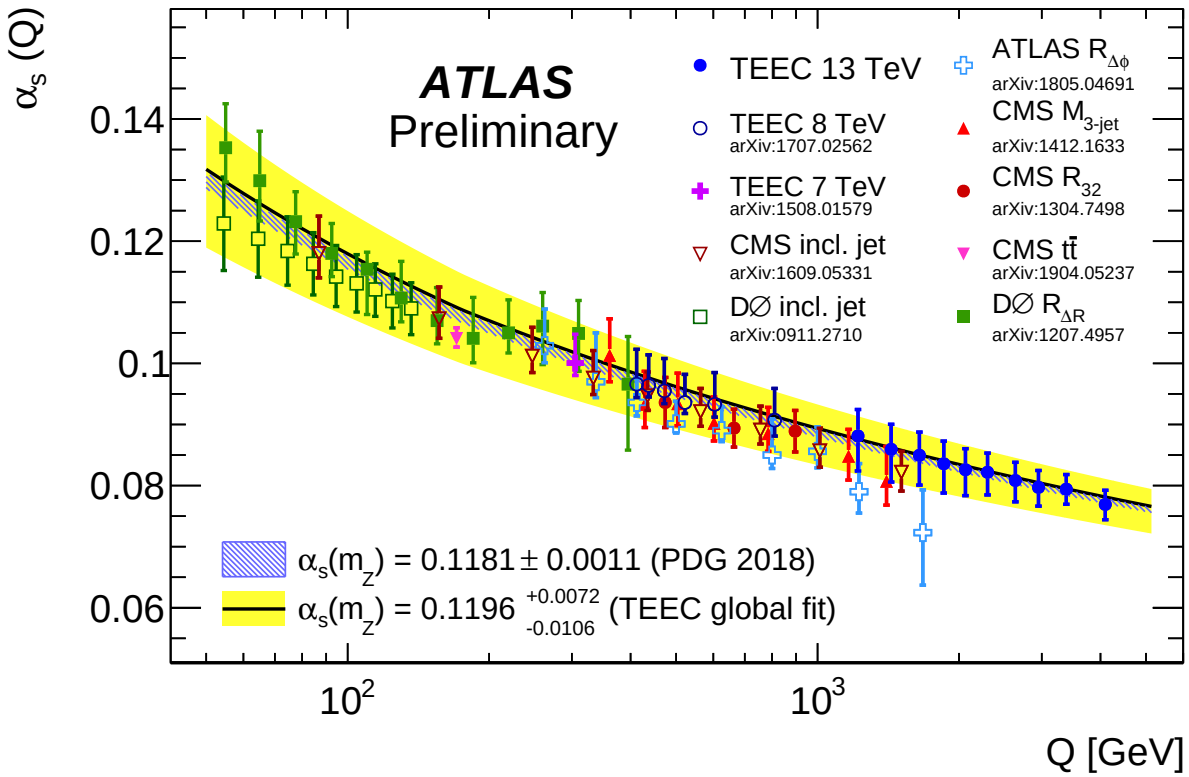

$\alpha_s(m_Z) = 0.1196 \pm 0.0001\ (\text{stat.}) \pm 0.0004\ (\text{sys.})^{+0.0071}_{-0.0104}\ (\text{scale}) \pm 0.0011\ (\text{PDF}) \pm 0.0002\ (\text{NP})$.

- Uncertainties dominated by μ-variations. PDFs and NP very small over H_{T2}.
- Total experimental uncertainties (stat. $\oplus$ syst.) are generally below 1%.

ATLAS diphoton cross section at $\sqrt{s} = 13$ TeV [JHEP 11, 169 (2021)]

- Measurement of $\gamma\gamma$ production for $p_T(\gamma_1) > 40$ GeV, $p_T(\gamma_2) > 30$ GeV.
- Direct, $H \to \gamma\gamma$ and fragmented γ signal, against non-prompt background.
- Background estimated from (ID, iso) sidebands for 2 photons (16 regions).
- Poisson likelihood fit performed separately on each bin of each observable.

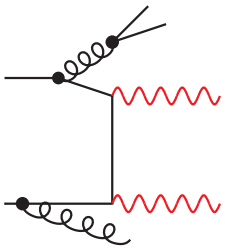

Direct photons

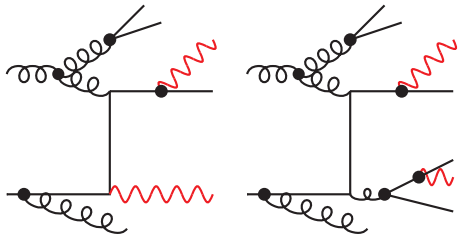

Fragmented photons

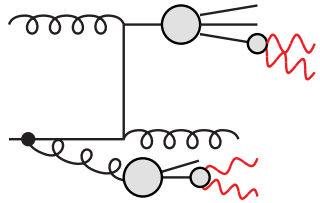

Non-prompt photons

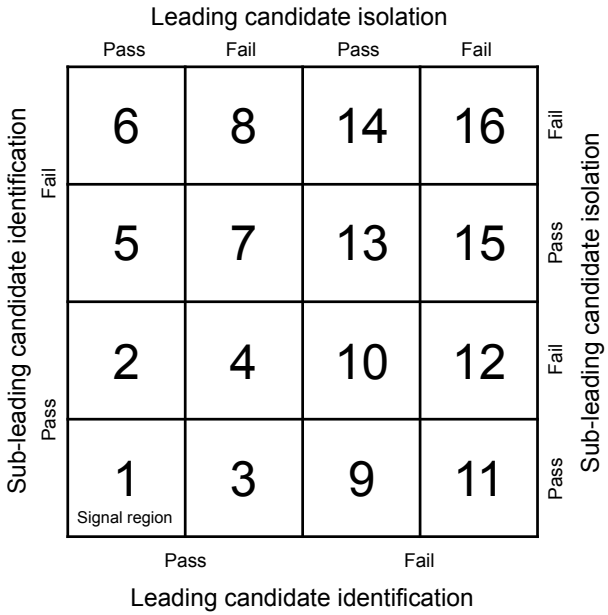

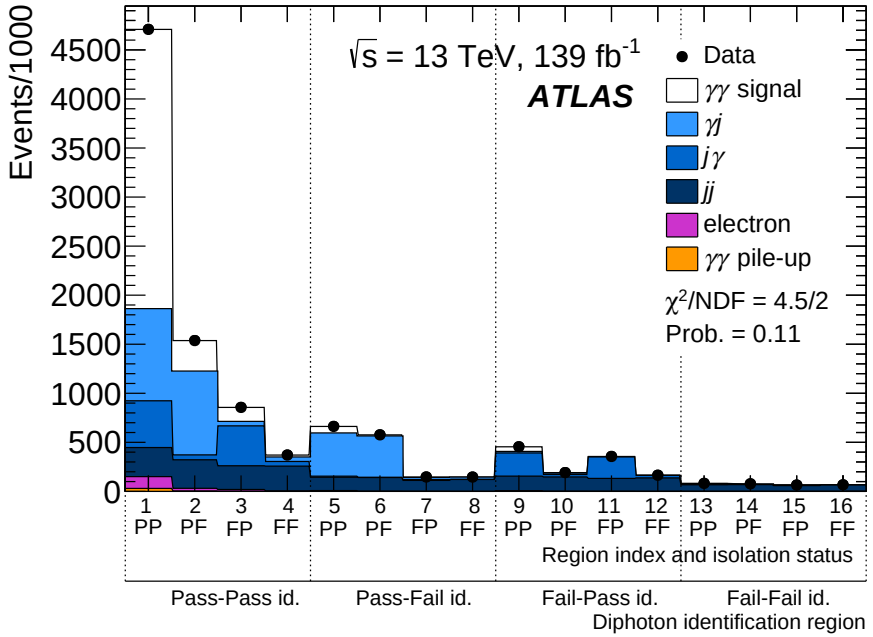

ATLAS diphoton cross section at $\sqrt{s} = 13$ TeV [JHEP 11, 169 (2021)]

- Comparison to ME+PS and fixed-order pQCD predictions.
- Sherpa (NLO+PS) and NNLOJet give a good description.
- NNLOJet fails in soft-log sensitive region at low-p_T.
- NNLOJet provides improved scale precision wrt NLO.
- DiPhox (NLO) fails to describe the data.

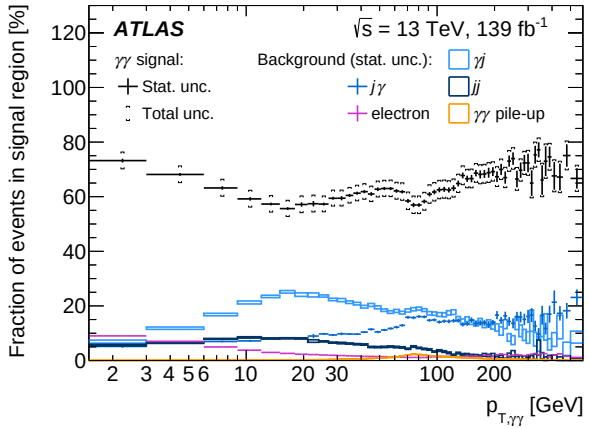

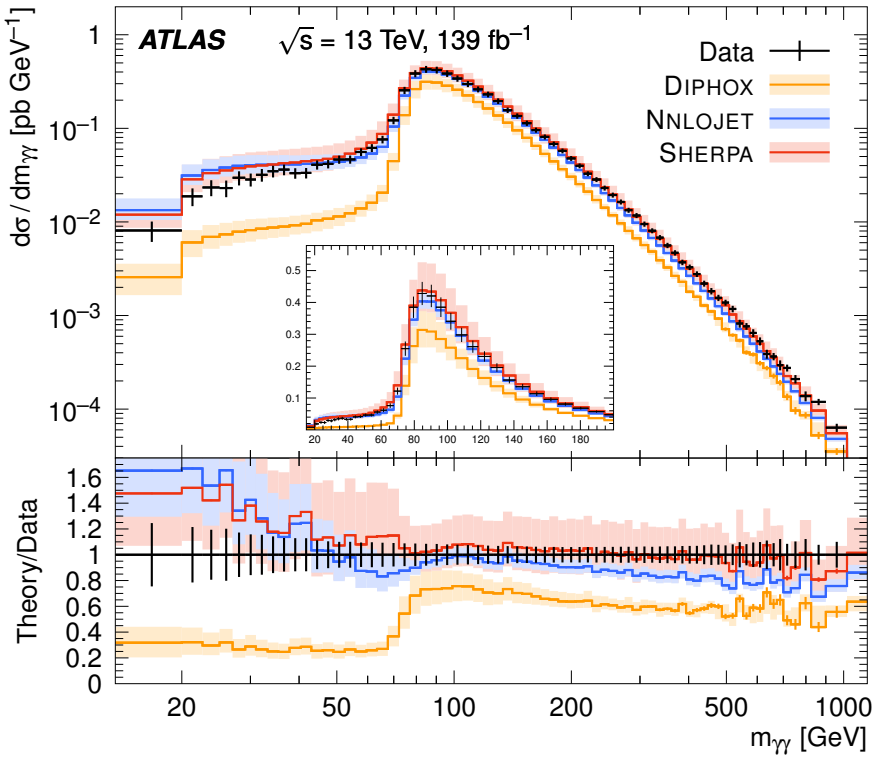

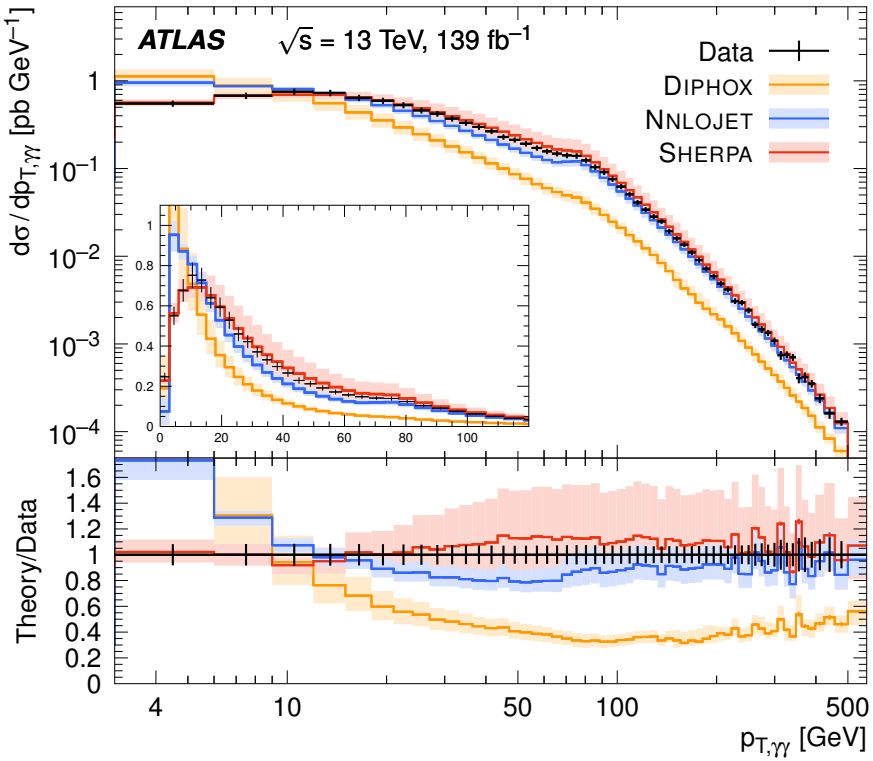

ATLAS b-fragmentation to $B^{\pm}$ at $\sqrt{s} = 13$ TeV [JHEP 12, 131 (2021)]

- Fragmentation observables for jets containing $B^{\pm} \to J/\psi K^{\pm}$ at $\Delta R < 0.4$
- Fully reconstructed decay from $\mu\mu K$ tracks.
- Longitudinal and transverse profiles of $B^{\pm}$:

$$z = \frac{\vec{p}_J \cdot \vec{p}_B}{|\vec{p}_J|^2}; \qquad p_T^{\mathrm{rel}} = \frac{|\vec{p}_J \times \vec{p}_B|}{|\vec{p}_J|}$$

- Background estimated using $M_{\mu\mu K}$ likelihood fits.

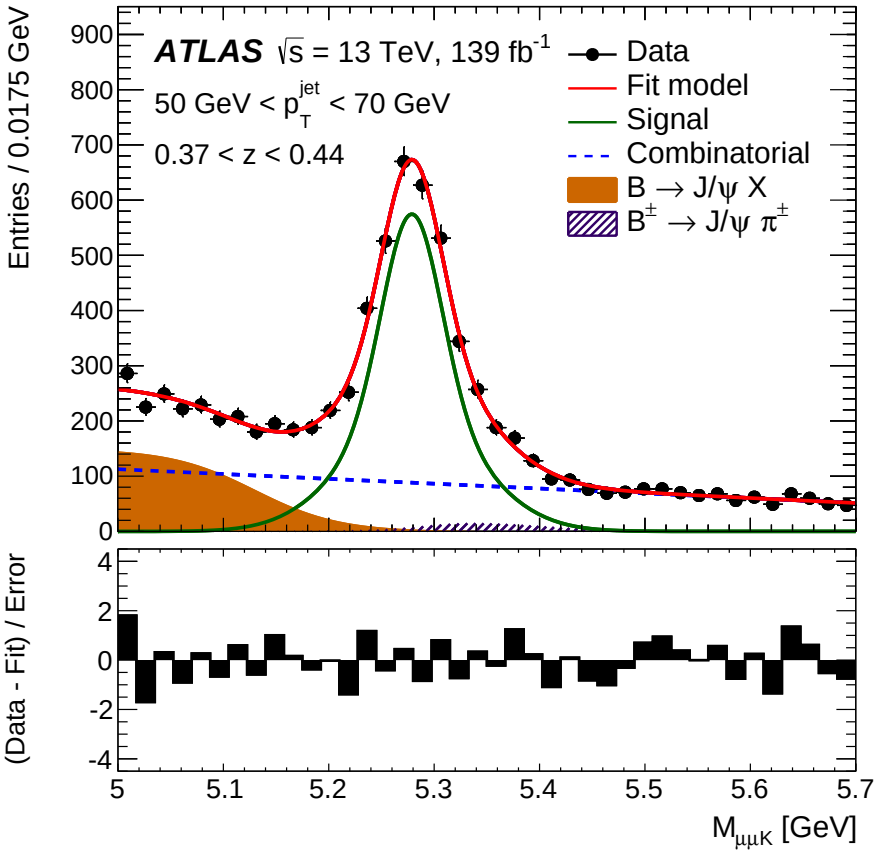

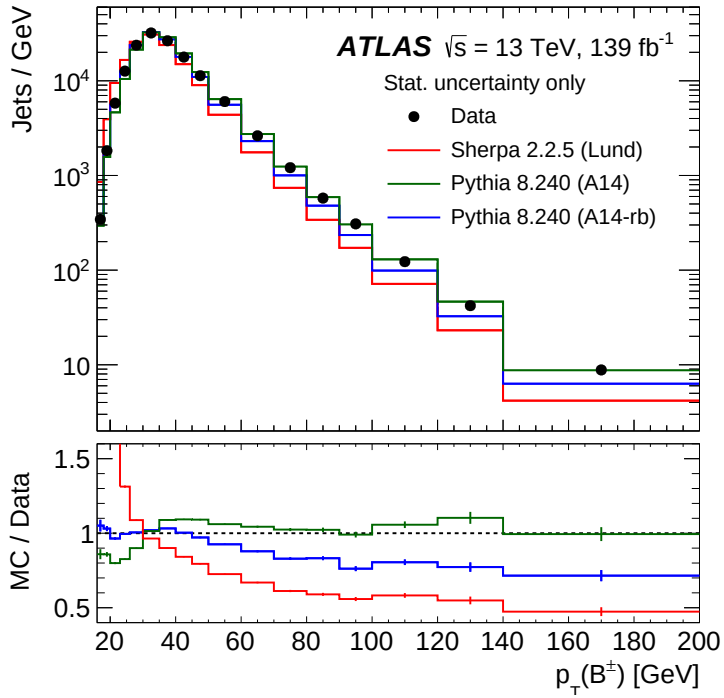

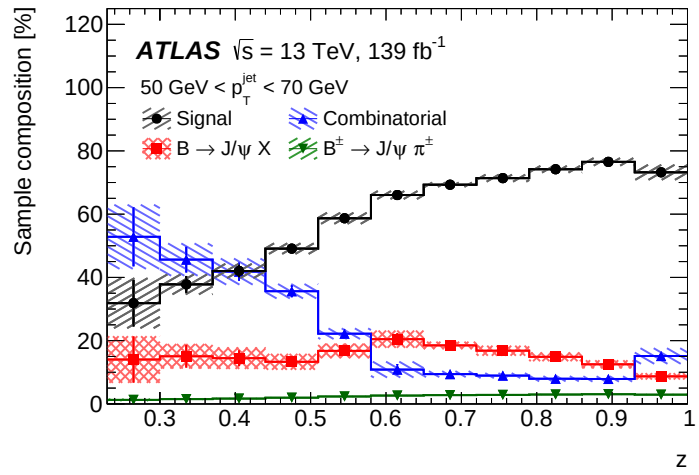

ATLAS b-fragmentation to $B^{\pm}$ at $\sqrt{s} = 13$ TeV [JHEP 12, 131 (2021)]

- Comparison to different ME+PS+fragmentation models.
- Pythia, Sherpa, H7 with different fragmentation/PS.
- Pythia A14-rb uses fitted $r_b = 1.05$ from LEP+SLD data.
- Sensitivity to $g \to b\bar{b}$ splitting is investigated.
- Discrepancies observed with H7 dipole shower ($g \to b\bar{b}$).
- Sherpa cluster model shows discrepancies at high z.

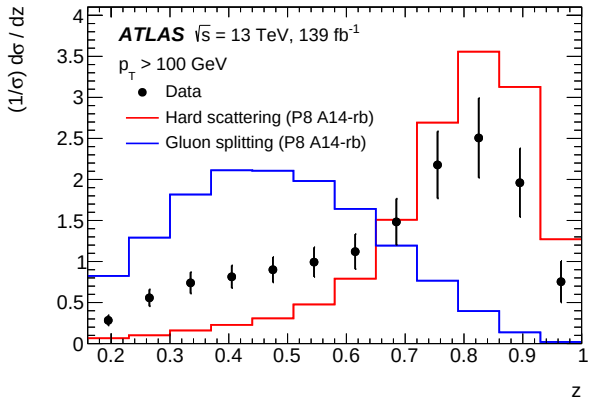

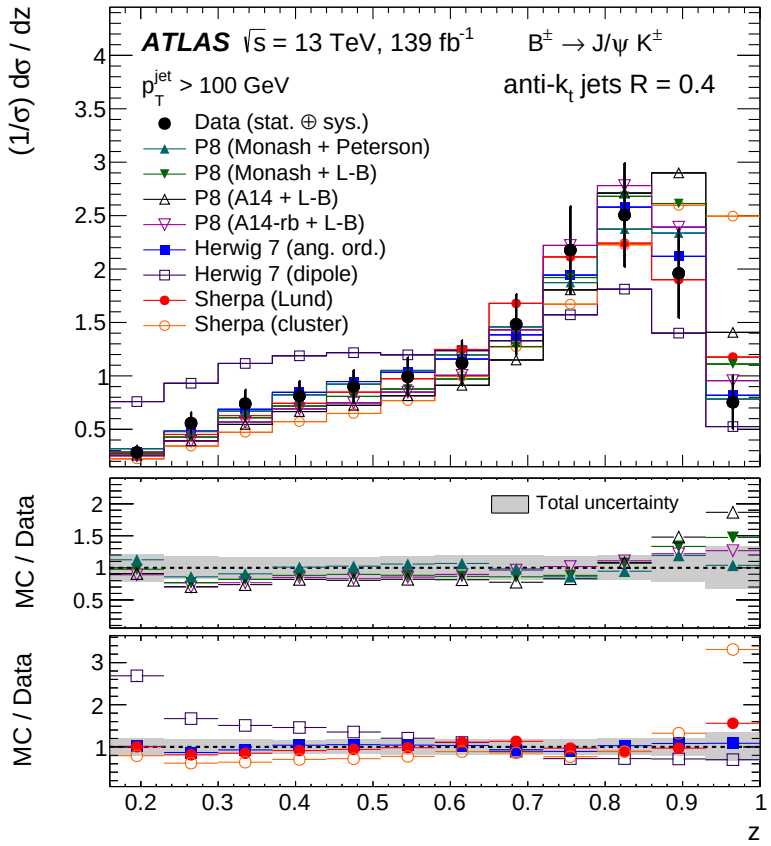

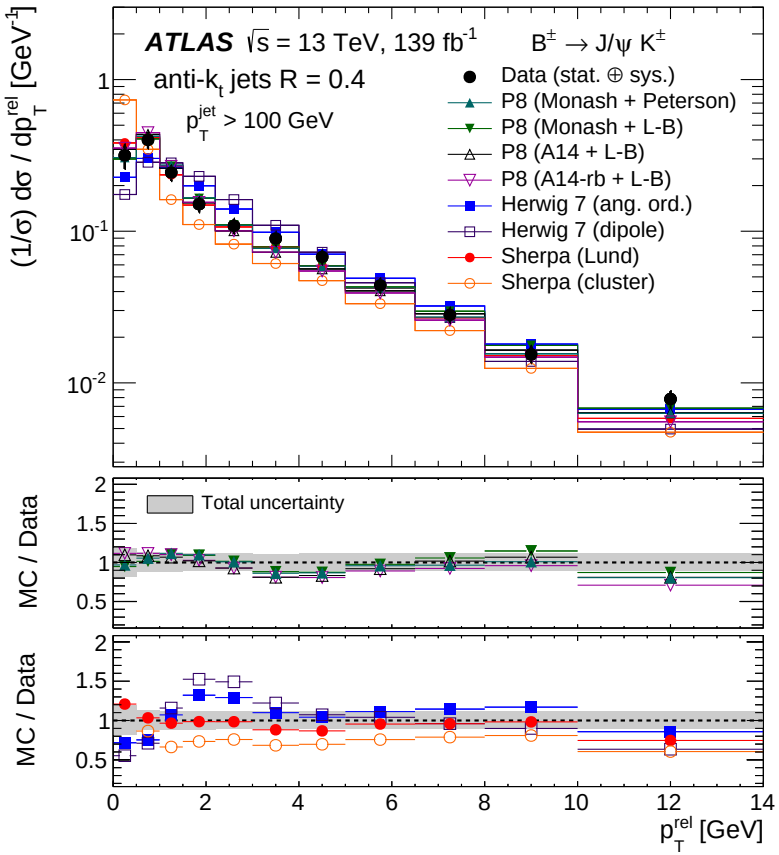

ATLAS b-fragmentation in $t\bar{t}$ at $\sqrt{s} = 13$ TeV [arXiv:2202.13901 (hep-ex)]

- Event selection in $t\bar{t} \to b\bar{b}e^{\pm}\mu^{\mp}$ dileptonic events.
- Exactly two jets: tag one jet, use the other as probe.
  - Probe jet should contain SV with at least 3 tracks.
  - If both jets are tagged, both jets are measured.
- Tracks from secondary vertex used to reconstruct $\vec{p}_b^{\,ch}$.
- All ghost-associated tracks used to reconstruct $\vec{p}_{jet}^{\,ch}$.

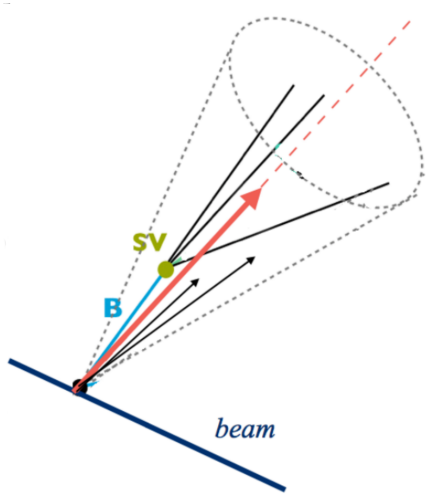

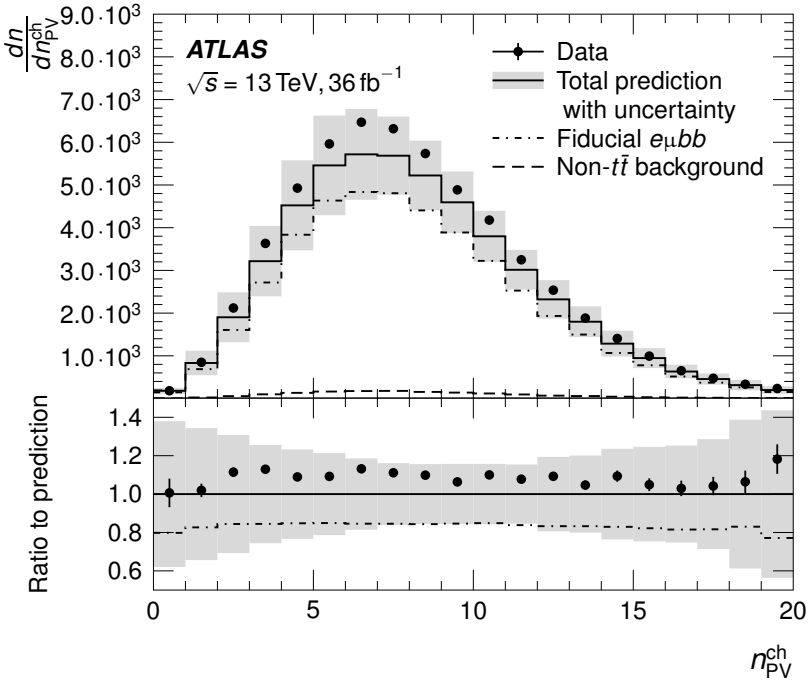

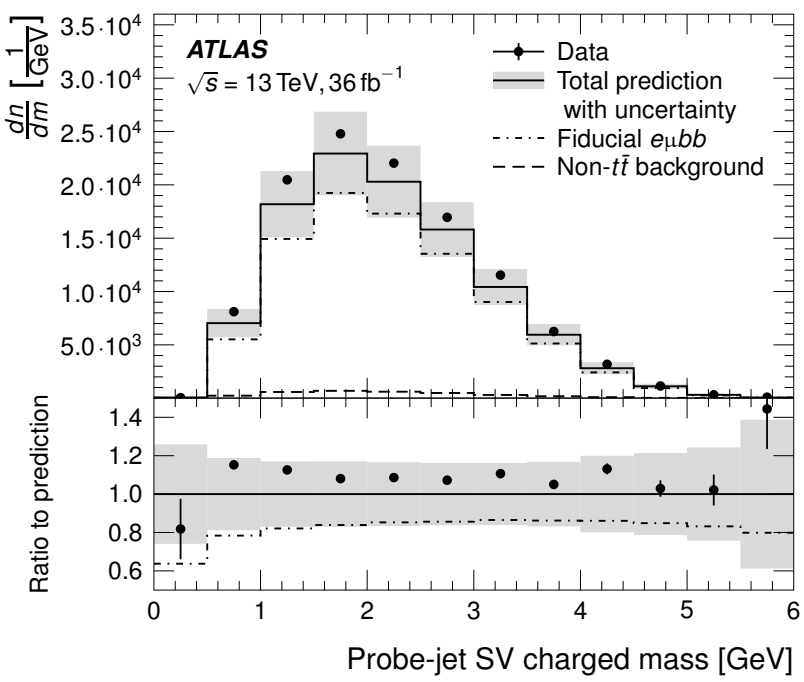

ATLAS b-fragmentation in $t\bar{t}$ at $\sqrt{s} = 13$ TeV [arXiv:2202.13901 (hep-ex)]

- Results are in reasonable agreement with MC expectations.
- Powheg + Pythia 8 gives a good description of the data.
- Powheg + Herwig 7.1.3 shows large differences at low z.
- Sherpa 2.2.10 provides the best overall description.

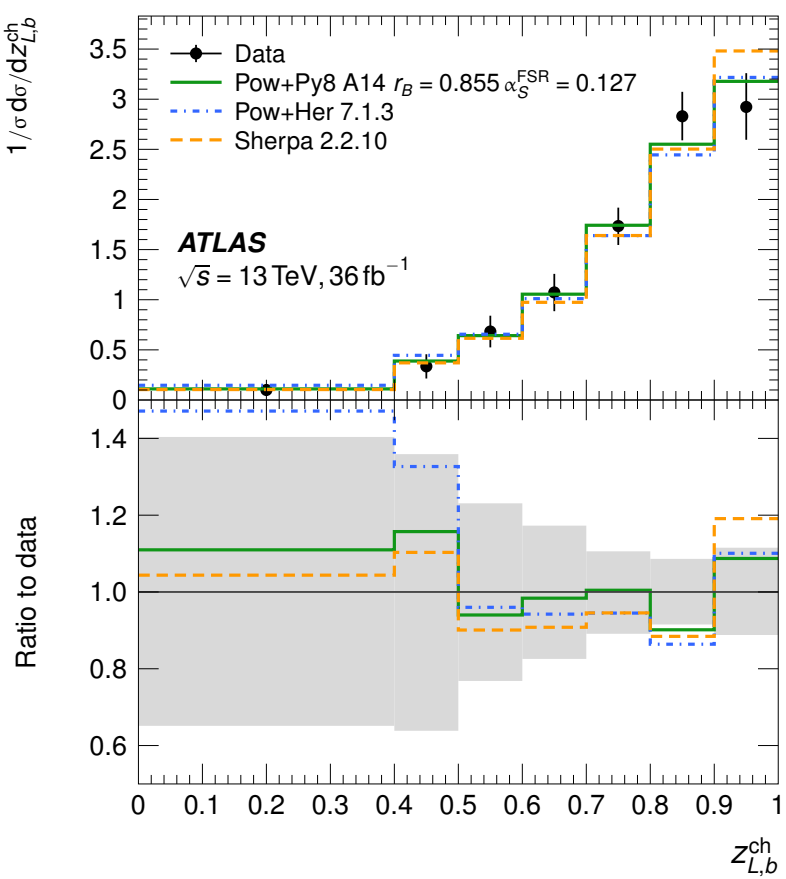

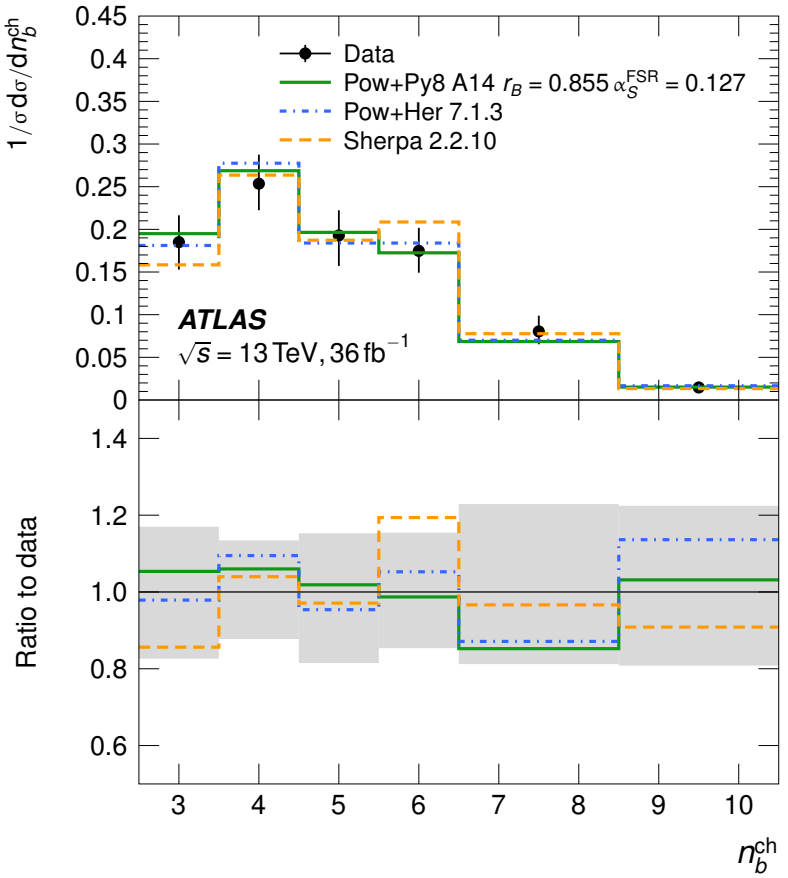

- Interesting dependence with α_s^{FSR}. No dependence with α_s^{ISR}.

Summary and conclusions

- Wide variety of QCD measurements recently released by ATLAS.
- Different analyses sensitive to different aspects of the QCD modelling.
- PDF fits have been performed using multiple ATLAS datasets.
- Z+jets and multijet final states are thoroughly explored.
- Diphoton cross section compared to theoretical predictions up to NNLO.
- b-quark fragmentation explored in two different final states.
  - In dijets with $B^{\pm}$ production, with explicit sensitivity to $g \to b\bar{b}$.
  - In $t\bar{t}$ using charged momentum of B-hadrons.
- Stay tuned for more interesting results!

Backup slides

ATLAS global PDF fit at $\sqrt{s} = 7$, 8, 13 TeV [EPJC 82, 438 (2022)]

Comparison of ATLAS PDF to global MSHT20, NNPDF, ABMP16 fits.

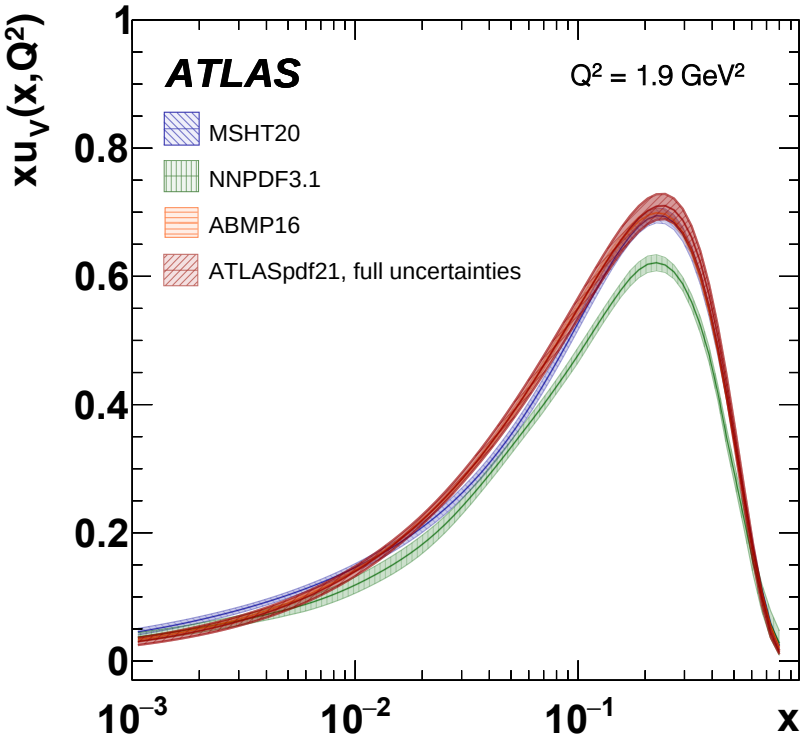

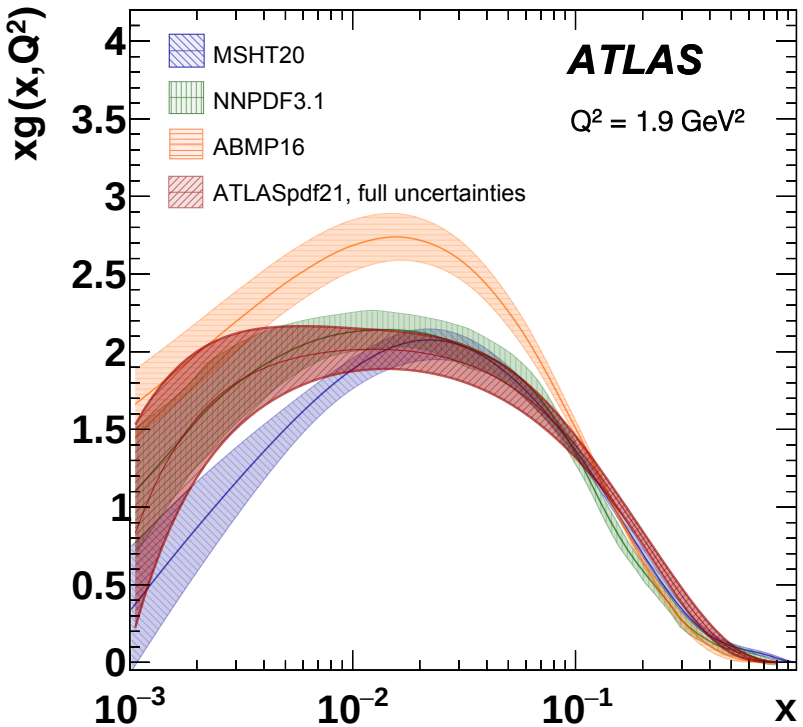

ATLAS b-fragmentation in $t\bar{t}$ at $\sqrt{s} = 13$ TeV [arXiv:2202.13901 (hep-ex)]

Dependence of $z_{L,b}^{\mathrm{ch}}$ and n_b^{ch} with α_s^{FSR}